Journal of Physics: Conference Series **2885** (2024) 012077 doi:10.1088/1742-6596/2885/1/012077

Simulation of Complete or Incomplete Biomass Degradation under Parameterized Wildland Fire Spread Conditions

Mohamed Mohsen Ahmed[a,b], **Hazem M. Al-Bulqini**[a], **Arnaud Trouvé**[a,*], **Jason Forthofer**[c], **Mark Finney**[c]

[a]Dept. of Fire Protection Engineering, University of Maryland, College Park, MD 20742, USA
[b]Materials Science Division, Lawrence Livermore National Lab., Livermore, CA 94550, USA
[c]USDA Forest Service, Missoula Fire Sciences Laboratory, Missoula, MT 59808, USA

E-mail: atrouve@umd.edu

Abstract. Our objective in the present study is to provide fundamental insights into the main factors that control the thermal degradation processes occurring inside the biomass vegetation during wildland fire spread. These processes determine the formation of flammable volatiles through pyrolysis reactions and the intensity of the internal heat release through char oxidation reactions; both aspects are central to flaming and smoldering combustion. We adopt here a simplified framework in which the biomass vegetation is viewed as a population of discrete elongated particles that are made of pine wood, are cylindrical-shaped and feature different diameters. The exposure conditions experienced by these particles in an assumed fire are characterized by a given intensity of the external thermal load, a given duration during which this load is applied, and a given external flow velocity that controls the rates of convective heat transfer and oxygen mass transfer. The response of the biomass particles is studied using a one-dimensional computational model, called the particle burning rate (PBR) model. The PBR model adopts a porous medium formulation, and provides a description of drying, (thermal and oxidative) pyrolysis, and char oxidation. We focus in the present study on the conditions required for complete "fuel consumption", *i.e.*, for complete particle degradation from virgin solid to ash. It is found that in thin biomass particles, complete biomass degradation requires sufficiently high intensities of the external thermal load and sufficiently low external flow velocities; high flow velocities correspond to excessive cooling effects. Similarly, in thick biomass particles, complete biomass degradation requires sufficiently high intensities of the external thermal load, sufficiently long application times of the thermal load, and sufficiently high external flow velocities; low flow velocities correspond to insufficient oxygenation of the (exothermic) oxidative pyrolysis and char oxidation reactions.

1. Introduction

Wildland fire spread results from complex interactions between external-gas processes taking place outside of the biomass and internal solid-gas processes taking place inside [1]. Relevant external-gas processes include turbulent mixing, flaming combustion and convective/radiative heat transfer; relevant internal biomass processes include pyrolysis and char oxidation reactions. Pyrolysis reactions are mostly endothermic and produce flammable volatiles, *i.e.*, the fuel for flaming combustion, whereas char oxidation reactions are strongly exothermic and produce conditions for self-sustained degradation. Note that char oxidation reactions are generally

referred to as smoldering combustion [2]. While the coupling between external-gas and internal solid-gas processes can be studied using Computational Fluid Dynamics (CFD) [3], there is significant value in trying to uncouple the controlling phenomena and in reducing the complexity of the fire spread problem by adopting the perspective of the biomass vegetation. In that perspective, fire spread is a repeated cycle of exposure to fire conditions and response in terms of release of flammable volatiles and heat to the surroundings. In the present study, we adopt the perspective of the biomass, specify the exposure conditions, and focus on the biomass response.

We consider that the biomass vegetation can be treated as a population of discrete elongated particles that are made of pine wood, are cylindrical-shaped and feature different diameters. The choice of pine wood as a representative dead fuel material is made for convenience and we recognize that the scope of the study could be extended by considering other biomass materials. The choice of a cylindrical shape for particles is an educated guess. In the present framework, the exposure conditions experienced by biomass particles in an assumed spreading fire are characterized by a given intensity of the external thermal load, a given duration during which this thermal load is applied, and a given external flow velocity that controls the rates of convective heat transfer and oxygen mass transfer.

The external thermal load is quantified by a new quantity called the "pseudo-incoming heat flux" (PIHF) [3]. PIHF is a heat flux variable that characterizes the intensity of the external thermal load without being obscured by the particle response. Recent CFD simulations of wildland fire spread suggest that the thermal exposure of a biomass particle can be quantified by a profile of large positive values taken by PIHF during a certain duration [3]. While this profile may take different shapes, we choose here to describe the temporal variations of PIHF as a step function characterized by a constant value, noted $\overline{\text{PIHF}}$, and a duration, noted τ_{PIHF}. In Ref. [3], the intense heating phase is defined as the period during which excess values of PIHF due to a passing fire (including both flaming and smoldering combustion) are greater than 10% of their peak value. $\overline{\text{PIHF}}$ represents the time-averaged value of PIHF during this intense heating phase; τ_{PIHF} represents the duration of that phase. In Ref. [3], representative values of $\overline{\text{PIHF}}$ are between 70 and 100 kW/m^2; representative values of τ_{PIHF} are between 20 and 40 s. In addition, representative values of the external flow velocity, noted $u_{g,\infty}$, are between 1 and 2 m/s.

The objective of the present study is to characterize the response of biomass particles of different diameters, noted d_p, to fire exposure conditions parametrized by $\overline{\text{PIHF}}$, τ_{PIHF} and $u_{g,\infty}$. We consider the following variations: $2 \leq d_p \leq 20$ mm; $10 \leq \overline{\text{PIHF}} \leq 120$ kW/m^2; $15 \leq \tau_{\text{PIHF}} \leq 60$ s; and $0 \leq u_{g,\infty} \leq 5$ m/s. Particles with $d_p = 2$ mm ($d_p = 20$ mm) are considered as representative of "thin" ("thick") biomass elements, *i.e.*, of biomass elements featuring weak (strong) temperature variations. We simulate the in-particle processes using an in-house one-dimensional computational model, called the particle burning rate (PBR) model. The PBR model is based on a framework developed by Lautenberger & Fernandez-Pello [4, 5]; the model adopts a porous medium formulation, provides a description of drying and thermal pyrolysis, and includes a description of in-depth oxygen mass diffusion, and exothermic oxidative pyrolysis and char oxidation reactions. We focus here on the conditions required for complete "fuel consumption", *i.e.*, complete particle degradation, or equivalently complete drying and pyrolysis from virgin solid to char, followed by complete char oxidation from char to ash.

2. The Particle Burning Rate (PBR) Model

We follow previous work in Ref. [4] and describe each fuel particle as a matrix of pores featuring a solid-phase and a gas-phase. The composition of the solid-phase of the particle is described in terms of four constituents: wet solid (ws), dry solid (ds), char (c) and ash (a); the composition of the gas-phase is described in terms of oxygen. The fuel particles are made of pine wood. We consider that each particle may experience four heterogeneous (gas/solid) reactions: a drying

reaction (*Rd*) that transforms *ws* into water vapor and *ds*; a thermal pyrolysis reaction (*Rp*) and an oxidative pyrolysis reaction (*Rop*) that transform *ds* into gaseous fuel (called volatiles) for the external flaming combustion process and *c*; and a char oxidation reaction (*Rco*) that transforms *c* into gaseous combustion products (treated as carbon dioxide CO_2) and *a*:

$$\text{Reaction } (Rd): \quad [\text{ws}] \longrightarrow \eta_{H_2O,Rd}\ [H_2O] + \eta_{ds,Rd}\ [\text{ds}] \tag{1}$$

$$\text{Reaction } (Rp): \quad [\text{ds}] \longrightarrow \eta_{v,Rp}\ [\text{volatiles}] + \eta_{c,Rp}\ \ [\text{c}] \tag{2}$$

$$\text{Reaction } (Rop): \quad [\text{ds}] + \eta_{O_2,Rop}[O_2] \longrightarrow \eta_{v,Rop}\ [\text{volatiles}] + \eta_{c,Rop}\ [\text{c}] \tag{3}$$

$$\text{Reaction } (Rco): \quad [\text{c}] + \eta_{O_2,Rco}\ [O_2] \longrightarrow \eta_{CO_2,Rco}\ [CO_2] + \eta_{a,Rco}\ [\text{a}] \tag{4}$$

where $\eta_{H_2O,Rd}$ and $\eta_{ds,Rd}$ are the mass yields of water vapor and dry solid in reaction (*Rd*), respectively; where $\eta_{v,Rp}$ and $\eta_{c,Rp}$ are the mass yields of volatiles and char in reaction (*Rp*), respectively; where $\eta_{O_2,Rop}$ is the oxygen-to-dry-solid mass ratio, and $\eta_{v,Rop}$ and $\eta_{c,Rop}$ are the mass yields of volatiles and char in reaction (*Rop*), respectively; and where $\eta_{O_2,Rco}$ is the oxygen-to-char mass ratio, and $\eta_{CO_2,Rco}$ and $\eta_{a,Rco}$ are the mass yields of carbon dioxide and ash in reaction (*Rco*), respectively. Reactions (*Rd*) and (*Rp*) require high enough temperatures and are endothermic; in contrast, reactions (*Rop*) and (*Rco*) require both high enough temperatures and the presence of oxygen, and are exothermic.

We follow the modeling choices made in Refs. [4, 5] and characterize each solid-phase constituent by a set of values for reference thermal properties and porous medium parameters; we also characterize each reaction by a set of values for chemical kinetics parameters. See Ref. [3] for modeling details and values of all input parameters.

While the PBR model developed in the present work can accommodate changes in particle volume, we follow Ref. [4] and treat each reaction, (*Rd*), (*Rp*), (*Rop*) and (*Rco*), as an iso-volumetric process. Furthermore, in-particle flow is treated as pressure-driven and uses Darcy's law. The model also assumes thermal equilibrium between the solid and gas phases and both phases are characterized by the same particle temperature [3].

In summary, the PBR model solves for four solid species mass equations (*ws*, *ds*, *c* and *a*), one temperature equation, one gaseous oxygen mass equation and one pressure equation. We solve the PBR equations using a one-dimensional formulation that can accommodate rectangular-, cylindrical- or spherical-shaped geometries; the present study considers cylindrical geometries. The PBR equations are integrated in time using an implicit iterative approach and an adaptive time resolution algorithm that controls the value of the time step to guarantee small incremental variations in the simulated particle temperature (typically no more than 0.1 K during each update of the solution). The PBR equations are discretized in space using a uniform computational mesh (the PBR solver features a re-meshing capability that is unused in the present study because the particles have constant volume). The spatial resolution used in the PBR model is $\Delta x_s = 10\ \mu$m. This high resolution was found to be necessary to avoid numerical instability problems and to accurately capture the stiff spatial variations associated with the char oxidation reaction (the thickness of the simulated char oxidation reaction zone can be as small as 0.1 mm). Additional information on the PBR model can be found in Ref. [3].

The PBR model uses several input parameters that characterize the environmental conditions in the ambient gas surrounding a given biomass particle: the incoming radiative heat flux, G; the temperature of the ambient gas, $T_{g,\infty}$; the magnitude of the flow velocity, $u_{g,\infty}$; and the oxygen mass fraction in the ambient gas, $Y_{g,O_2,\infty}$. These parameters appear in the boundary conditions of the PBR equations, for instance in the expressions for the external-gas-to-particle heat flux, $\dot{q}''_{g\to p}$, and the external-gas-to-particle oxygen mass flux, $\dot{m}''_{O_2,g\to p}$. In these expressions, the convective heat transfer coefficient, h, plays a central role [3]. The PBR model for h first starts from Ref. [4] where h is described as a baseline reference value, h_{ref}, modified by blowing effects.

The PBR model also deviates from Ref. [4] and treats h_{ref} through standard, Nusselt-number-based, engineering correlations [6]:

$$h_{ref} = \mathrm{Nu}_{d_p} \times \frac{k_g}{d_p} \tag{5}$$

where Nu_{d_p} is the Nusselt number of the particle (based on the particle diameter), and k_g the heat conductivity of the gas evaluated at the film temperature. The Nusselt number is obtained from one of the recommended correlations found in the heat transfer literature [6]:

$$\mathrm{Nu}_{d_p} = 0.3 + \frac{0.62 \times \mathrm{Re}_{d_p}^{0.5} \times Pr^{1/3}}{\left(1 + \left(\frac{0.4}{Pr}\right)^{2/3}\right)^{1/4}} \left(1 + \left(\frac{\mathrm{Re}_{d_p}}{282000}\right)^{5/8}\right)^{4/5} \tag{6}$$

where Re_{d_p} is the Reynolds number of the particle and Pr the Prandtl number, all properties being evaluated at the film temperature.

The expressions in Eqs. (5) and (6) make h a strong function of the external flow velocity and particle diameter: consistent with previous experimental observations [7, 8], "thick" biomass particles ($d_p > 10$ mm) feature moderate values of the convective heat transfer coefficient, *i.e.*, $h < 50$ W/m^2/K, and are therefore only weakly sensitive to convective heating and cooling, while "thin" biomass particles ($d_p < 10$ mm) feature high values of the convective heat transfer coefficient, *i.e.*, $h > 100$ W/m^2/K (provided that $u_{g,\infty} > 1.5$ m/s), and are strongly sensitive to convective heating and cooling.

Furthermore, the number of input parameters in the PBR model can be reduced by introducing the concept of the "pseudo incoming heat flux", which is defined as the part of $\dot{q}''_{g\to p}$ that depends on external parameters and does not depend on the particle response [3]:

$$\mathrm{PIHF} = h \times T_{g,\infty} + \epsilon_{p,surf} \times G \tag{7}$$

where $\epsilon_{p,surf}$ is the emissivity of the particle surface. PIHF conveniently combines the convective and radiative components of heat transfer into a single quantity. Note that the concept that leads to PIHF is similar to that of an "adiabatic surface temperature" (AST) occasionally used in heat transfer applications, *e.g.*, in problems of fire-structure interactions [9].

In the present study, PIHF is described as a step function characterized by a constant value, noted $\overline{\mathrm{PIHF}}$, and a duration, noted τ_{PIHF}. Fire exposure conditions are then characterized through the following 3 parameters: $\overline{\mathrm{PIHF}}$, τ_{PIHF}, and h (where h is a function of $u_{g,\infty}$ and d_p, see Eqs. (5)-(6). In the present study, $Y_{g,O_2,\infty}$ is treated as equal to its value in air.

3. Results

We focus in the present study on the degree of completion of the thermal degradation process of individual biomass particles, noted η_p. η_p can be defined in several ways; we use here a total-solid-mass-based definition: $\eta_p = (m_0 - m_\infty)/(m_0 - m_{\infty,th})$, where m_0 (m_∞) is the initial (final) particle mass, and $m_{\infty,th}$ is the theoretical value of the final particle mass under complete particle degradation conditions, $m_{\infty,th} = m_0 \times (\eta_{ds,Rd}\ \eta_{c,Rp}\ \eta_{a,Rco})$; note that this expression of $m_{\infty,th}$ uses the assumption made in the pine wood model that the mass yields of char in reactions (Rp) and (Rop) are identical, $\eta_{c,Rp} = \eta_{c,Rop}$ [4].

Figure 2(a) presents the variations of η_p with $\overline{\mathrm{PIHF}}$ and $u_{g,\infty}$ for $d_p = 2$ mm and $\tau_{\mathrm{PIHF}} = 30$ s. The map is generated from a series of 88 PBR simulations with incremental variations in $\overline{\mathrm{PIHF}}$ and in $u_{g,\infty}$ equal to 10 or 20 kW/m^2, and 0.5 m/s, respectively (while smaller variations would lead to smoother contours, the present choice is deemed sufficient to capture the main features of changes in η_p). The grey region on the upper left corner of

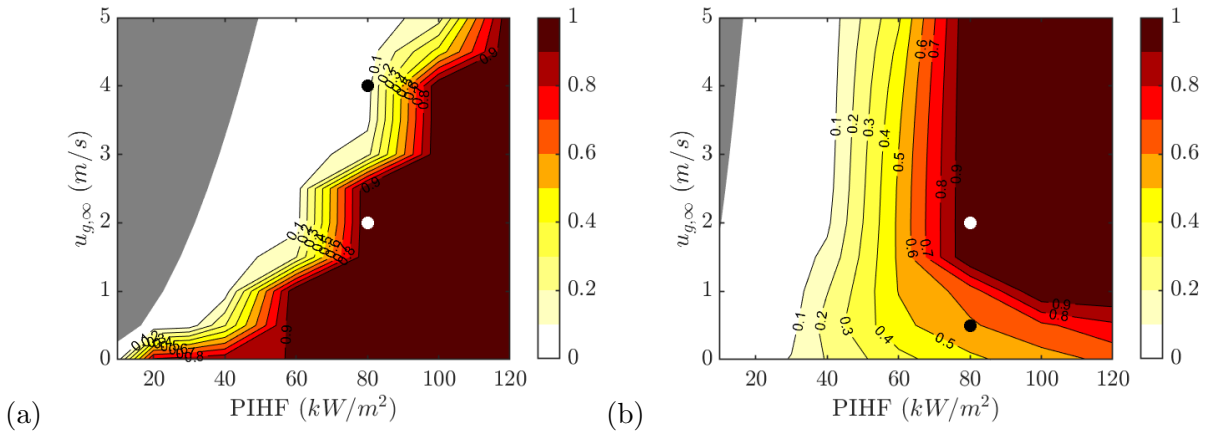

Figure 1. Variations of the degree of completion of the thermal degradation process, η_p, with $\overline{\text{PIHF}}$ and $u_{g,\infty}$.(a) $d_p = 2$ mm and $\tau_{\text{PIHF}} = 30$ s; (b) $d_p = 20$ mm and $\tau_{\text{PIHF}} = 60$ s.

the plot corresponds to values of $\overline{\text{PIHF}}$ that are smaller than the reference ambient value, $\overline{\text{PIHF}} < \text{PIHF}_0$, where $\text{PIHF}_0 = (h \times T_{g,0} + \epsilon_{p,surf} \times \sigma T_{g,0}^4)$, with $T_{g,0}$ the ambient air temperature, and that are therefore not physical and should be ignored. Figure 2(a) shows that for thin particles, complete thermal degradation ($\eta_p \approx 1$) occurs for sufficiently high values of $\overline{\text{PIHF}}$, $\overline{\text{PIHF}}_{min} < \overline{\text{PIHF}}$, and for sufficiently low values of $u_{g,\infty}$, $u_{g,\infty} < u_{g,max}$. We find in Figure 2(a) that: $\overline{\text{PIHF}}_{min} \approx 60$ kW/m^2; and $u_{g,max}$ is an increasing function of $\overline{\text{PIHF}}$. The low-$\overline{\text{PIHF}}$ limit is explained by the observation that reactions (*Rd*), (*Rp*), (*Rop*) and (*Rco*) are thermally-driven and that complete pyrolysis requires temperatures above 600 K, while complete char oxidation requires temperatures above 700 K. The high-$u_{g,\infty}$ limit is explained by excessive convective cooling observed at large values of the flow velocity.

Figure 2(b) presents similar variations for $d_p = 20$ mm and $\tau_{\text{PIHF}} = 60$ s. We consider here a longer application time of the thermal load because for $\tau_{\text{PIHF}} = 30$ s, $\eta_p << 1$ across most of the present parameter space. This evolution towards lower degrees of particle degradation when d_p is increased is explained by the longer in-particle diffusion times and by the presence of a cold core at the end of the heating period, and is consistent with the well-known observation that low-to-moderate-intensity fires will fully consume thin biomass elements while causing limited damage in thick biomass elements. Figure 2(b) shows that for "thick" particles, complete degradation ($\eta_p \approx 1$) occurs for sufficiently high values of $\overline{\text{PIHF}}$, $\overline{\text{PIHF}}_{min} < \overline{\text{PIHF}}$, and for sufficiently high values of $u_{g,\infty}$, $u_{g,min} < u_{g,\infty}$. We find in Figure 2(b) that: $\overline{\text{PIHF}}_{min} \approx 80$ kW/m^2; and $u_{g,min} \approx 1$ m/s. The low-$\overline{\text{PIHF}}$ limit is again explained by the need to raise the particle temperatures to values above 700 K. The low-$u_{g,\infty}$ limit is explained by insufficient oxygen mass transfer.

The dots seen in Figure 2(a)-(b) mark the conditions of cases that will be discussed in more detail during the oral presentation: Case 1 with $d_p = 2$ mm, $\tau_{\text{PIHF}} = 30$ s, $\overline{\text{PIHF}} = 80$ kW/m^2, $u_{g,\infty} = 2$ m/s; Case 2 with identical choices except that $u_{g,\infty} = 4$ m/s; Case 3 with $d_p = 20$ mm, $\tau_{\text{PIHF}} = 60$ s, $\overline{\text{PIHF}} = 80$ kW/m^2, $u_{g,\infty} = 2$ m/s; Case 4 with identical choices except that $u_{g,\infty} = 0.5$ m/s.

4. Conclusion

This study presents a computational analysis of the biomass response to the transient application of a thermal load due to a passing fire. The response of biomass elements, called particles, is parametrized in terms of a characteristic thickness of the particles, a given intensity of the

external thermal load, a given duration during which this load is applied, and a given external flow velocity that controls the rates of convective heat transfer and oxygen mass transfer. The external thermal load is quantified by a new quantity called the "pseudo-incoming heat flux" (PIHF) that characterizes the intensity of the external thermal load without being obscured by the particle response; PIHF is similar to the "adiabatic surface temperature" (AST) used in problems of fire-structure interactions.

The response of the biomass particles is studied using a one-dimensional computational model, called the particle burning rate (PBR) model. The PBR model adopts a porous medium formulation, includes a description of drying, thermal and oxidative pyrolysis, and char oxidation, as well as a description of the external-gas-to-particle diffusion of oxygen mass; the PBR model thereby provides a treatment of in-depth oxidative processes and allows the simulation of smoldering combustion.

We focus in the present study on the conditions required for complete "fuel consumption", *i.e.*, for complete particle degradation from virgin solid to ash. It is found that in thin biomass particles, complete biomass degradation requires sufficiently high intensities of PIHF and sufficiently low external flow velocities; high flow velocities correspond to excessive cooling effects. Similarly, in thick biomass particles, complete biomass degradation requires sufficiently high intensities of PIHF, sufficiently long application times of PIHF, and sufficiently high external flow velocities; low flow velocities correspond to insufficient oxygenation of the (exothermic) oxidative pyrolysis and char oxidation reactions. The key feature in the complete degradation of thick particles is the transition from pyrolysis, assisted by external heating, to self-sustained exothermic char oxidation. The PBR model captures that transition.

Finally, it is found that under most conditions, char oxidation is a rate-limited by oxygen diffusion and occurs in a thin region of sub-millimeter size. We recommend using a spatial resolution of 10-20 μm to correctly capture these stiff variations.

Acknowledgments

This project is financially supported by the USDA Forest Service, Missoula Fire Sciences Laboratory, and is also supported by supercomputing resources made available by the University of Maryland (*https://www.glue.umd.edu/hpcc/*) and by the US National Science Foundation (ACCESS Program, Grant # TG-CTS140046, *https://access-ci.org*). For the first author (M.M.A.), time for preparation of this manuscript was provided under the auspices of the US DOE by Lawrence Livermore National Laboratory under Contract DE-AC52-07NA27344.

References

[1] Finney M.A., McAllister S.S., Grumstrup T.P., Forthofer J.M., Wildland Fire Behavior - Dynamics, Principles and Processes, CSIRO Publishing, 2021.
[2] Rein G., Smoldering Combustion. In SFPE Handbook of Fire Protection Engineering, 5th Ed., Chapter 19, pp. 581-603, 2016.
[3] Ahmed M.M., Trouvé A., Finney M.A., Forthofer J.M. (2024) Simulations of flaming combustion and flaming-to-smoldering transition in wildland fire spread at flame scale, Combust. Flame 262:113370.
[4] Lautenberger C., Fernandez-Pello C. (2009) A model for the oxidative pyrolysis of wood, Combust. Flame 156:1503-1513.
[5] Lautenberger C., Fernandez-Pello C. (2009) Generalized pyrolysis model for combustible solids, Fire Saf. J. 44:819-839.
[6] Churchill S.W., Bernstein M. (1977) A correlating equation for forced convection from gases and liquids to a circular cylinder in crossflow, J. Heat Transfer 99:300-306.
[7] Finney M.A., Cohen J.D., McAllister S.S., Jolly W.M. (2013) On the need for a theory of wildland fire spread, Int. J. Wildland Fire 22:25-36.
[8] McAllister S., Finney M. (2017) Autoignition of wood under combined convective and radiative heating, Proc. Combust. Inst. 36:3073-3080.
[9] Wickström U. (2011) The adiabatic surface temperature and the plate thermometer, International Association for Fire Safety Science, Proc. 10th Intl. Symp., 1001-1012.